Article

Reactions of the Peroxo Intermediate of Soluble Methane Monooxygenase Hydroxylase with Ethers

Laurance G. Beauvais, and Stephen J. Lippard

J. Am. Chem. Soc., **2005**, 127 (20), 7370-7378• DOI: 10.1021/ja050865i • Publication Date (Web): 27 April 2005

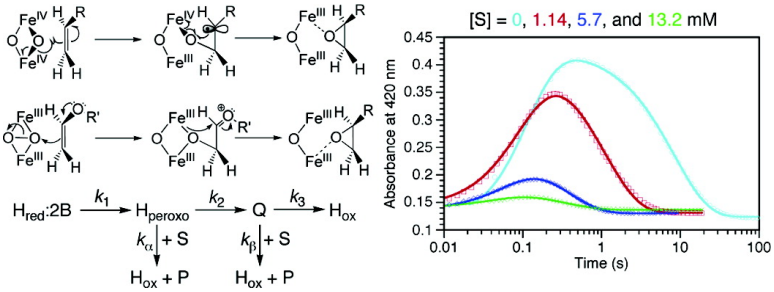

More About This Article

Additional resources and features associated with this article are available within the HTML version:

- Supporting Information
- Links to the 9 articles that cite this article, as of the time of this article download
- Access to high resolution figures
- Links to articles and content related to this article
- Copyright permission to reproduce figures and/or text from this article

View the Full Text HTML

J|A|C|S
ARTICLES
Published on Web 04/27/2005

Reactions of the Peroxo Intermediate of Soluble Methane Monooxygenase Hydroxylase with Ethers

Laurance G. Beauvais and Stephen J. Lippard*

Contribution from the Department of Chemistry, Massachusetts Institute of Technology, Cambridge, Massachusetts 02139

Received February 9, 2005; E-mail: lippard@mit.edu

Abstract: Soluble methane monooxygenase (sMMO) isolated from *Methylococcus capsulatus* (Bath) utilizes a carboxylate-bridged diiron center and dioxygen to catalyze the conversion of methane to methanol. Previous studies revealed that a di(μ-oxo)diiron(IV) intermediate termed Q is responsible for the catalytic activity with hydrocarbons. In addition, the peroxodiiron(III) intermediate (H_{peroxo}) that precedes Q formation in the catalytic cycle has been demonstrated to react with propylene, but its reactivity has not been extensively investigated. Given the burgeoning interest in the existence of multiple oxidants in metalloenzymes, a more exhaustive study of the reactivity of H_{peroxo} was undertaken. The kinetics of single turnover reactions of the two intermediates with ethyl vinyl ether and diethyl ether were monitored by single- and double-mixing stopped-flow optical spectroscopy. For both substrates, the rate constants for reaction with H_{peroxo} are greater than those for Q. An analytical model for explaining the transient kinetics is described and used successfully to fit the observed data. Activation parameters were determined through temperature-dependent studies, and the kinetic isotope effects for the reactions with diethyl ether were measured. The rate constants indicate that H_{peroxo} is a more electrophilic oxidant than Q. We propose that H_{peroxo} reacts via two-electron transfer mechanisms, and that Q reacts by single-electron transfer steps.

Introduction

Mechanistic studies of metalloenzymes have expanded our understanding of how nature utilizes a small set of metals and ligands to perform a wide variety of tasks. In the case of oxygenases, much more complicated catalytic cycles have emerged than were first envisioned.[1] For example, the long accepted radical rebound mechanism mediated by the Fe^{IV}═O porphyrin cation radical (Cpd I) in cytochrome P450 reactions[2] has been challenged by the proposal that an Fe(III)−hydroperoxo intermediate (Cpd 0), which precedes formation of Cpd I, can serve as a second, electrophilic oxidant. Evidence for a second oxidant derives from product distribution and kinetic isotope effects for reactions of wild-type P450 enzymes.[1d,e,3] An alternative explanation has been proposed for these results, namely, that Cpd I exists in both low and high spin states, each of which reacts by a different mechanism.[1b,4] An experimental resolution of this controversy suffers from the lack of an appropriate spectroscopic technique to monitor the reactions of the two intermediates, which cannot be deconvoluted by transient kinetics studies.

Multiple oxidizing species also occur in synthetic analogues of dicopper-containing hydroxylases.[1c] A (μ-η^2:η^2)peroxodicopper(II) center is assigned as the active oxidant in biological systems,[5] but small molecule mimics reveal a diverse range of peroxodicopper(II) and di(μ-oxo)dicopper(III) species.[1c,6] The relative energies of the peroxo and oxo forms can be modulated by judicious choice of supporting ligands.[1c] Intermediates in the activation of dioxygen by dicopper complexes can be observed by stopped-flow optical spectroscopy. A similar situation obtains for reactions of dioxygen with carboxylate-bridged diiron proteins, in which peroxodiiron(III), di(μ-oxo)diiron(III,IV), and diiron(IV) intermediates have been detected. Soluble methane monooxygenase (sMMO), an enzyme system

(1) The role of multiple intermediates in enzyme-catalyzed reactions was recently reviewed in a series of articles: (a) Que, L., Jr. *J. Biol. Inorg. Chem.* **2004**, *9*, 643. (b) Shaik, S.; de Visser, S. P.; Kumar, D. *J. Biol. Inorg. Chem.* **2004**, *9*, 661−668. (c) Hatcher, L. Q.; Karlin, K. D. *J. Biol. Inorg. Chem.* **2004**, *9*, 669−683. (d) Nam, W.; Ryu, Y. O.; Song, W. J. *J. Biol. Inorg. Chem.* **2004**, *9*, 654−660. (e) Jin, S.; Bryson, T. A.; Dawson, J. H. *J. Biol. Inorg. Chem.* **2004**, *9*, 644−653. (f) Que, L., Jr. *J. Biol. Inorg. Chem.* **2004**, *9*, 684−690.

(2) (a) Guengerich, F. P.; Macdonald, T. L. *Acc. Chem. Res.* **1984**, *17*, 9−16. (b) Sono, M.; Roach, M. P.; Coulter, E. D.; Dawson, J. H. *Chem. Rev.* **1996**, *96*, 2841−2887. (c) Groves, J. T. *Proc. Natl. Acad. Sci. U.S.A.* **2003**, *100*, 3569−3574.

(3) Selected references: (a) Vaz, A. D. N.; Pernecky, S. J.; Raner, G. M.; Coon, M. J. *Proc. Natl. Acad. Sci. U.S.A.* **1996**, *93*, 4644−4648. (b) Vaz, A. D. N.; McGinnity, D. F.; Coon, M. J. *Proc. Natl. Acad. Sci. U.S.A.* **1998**, *95*, 3555−3560. (c) Zakharieva, O.; Trautwein, A. X.; Veeger, C. *Biophys. Chem.* **2000**, *88*, 11−34. (d) Volz, T. J.; Rock, D. A.; Jones, J. P. *J. Am. Chem. Soc.* **2002**, *124*, 9724−9725. (e) Vatsis, K. P.; Coon, M. J. *Arch. Biochem. Biophys.* **2002**, *397*, 119−129. (f) Newcomb, M.; Hollenberg, P. F.; Coon, M. J. *Arch. Biochem. Biophys.* **2003**, *409*, 72−79. (g) Newcomb, M.; Aebisher, D.; Shen, R.; Chandrasena, R. E. P.; Hollenberg, P. F.; Coon, M. J. *J. Am. Chem. Soc.* **2003**, *125*, 6064−6065. (h) Jin, S.; Makris, T. M.; Bryson, T. A.; Sligar, S. G.; Dawson, J. H. *J. Am. Chem. Soc.* **2003**, *125*, 3406−3407.

(4) Selected references: (a) Shaik, S.; de Visser, S. P.; Ogliaro, F.; Schwarz, H.; Schröder, D. *Curr. Opin. Chem. Biol.* **2002**, *6*, 556−567. (b) Ogliaro, F.; de Visser, S. P.; Cohen, S.; Sharma, P. K.; Shaik, S. *J. Am. Chem. Soc.* **2002**, *124*, 2806−2817. (c) Sharma, P. K.; de Visser, S. P.; Shaik, S. *J. Am. Chem. Soc.* **2003**, *125*, 8698−8699. (d) Kamachi, T.; Shiota, Y.; Ohta, T.; Yoshizawa, K. *Bull. Chem. Soc. Jpn.* **2003**, *76*, 721−732.

(5) (a) Decker, H.; Dillinger, R.; Tuczek, F. *Angew. Chem., Int. Ed.* **2000**, *39*, 1591−1595. (b) Yamazaki, S.-i.; Itoh, S. *J. Am. Chem. Soc.* **2003**, *125*, 13034−13035. (c) Yamazaki, S.-i.; Morioka, C.; Itoh, S. *Biochemistry* **2004**, *43*, 11546−11553.

(6) Que, L., Jr.; Tolman, W. B. *Angew. Chem., Int. Ed.* **2002**, *41*, 1114−1137.

10.1021/ja050865i CCC: $30.25

Scheme 1

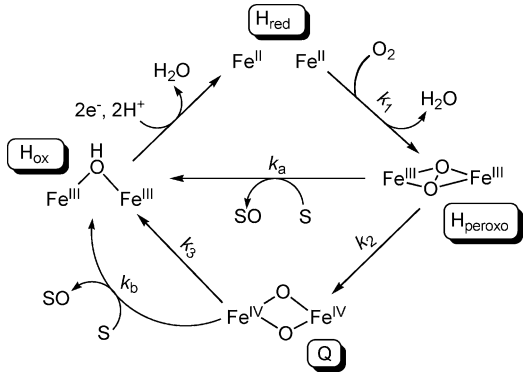

that converts methane to methanol in methanotrophic bacteria, is unique among wild-type carboxylate-bridged diiron proteins, in that both (peroxo)diiron(III) (H_{peroxo}) and high-valent di(μ-oxo)diiron(IV) (Q) intermediates have sufficiently long lifetimes and extinction coefficients to be followed by stopped-flow optical spectroscopy.[7] Thus, sMMO is well suited for studying the role of multiple oxidants in a biological system.

sMMO isolated from *Methylococcus capsulatus* (Bath) (*Mc*) and *Methylosinus trichosporium* OB3b (*Mt*) have been extensively investigated. Substrate hydroxylation occurs at a carboxylate-bridged diiron center residing in the α subunit of the hydroxylase protein MMOH, a 251 kDa $\alpha_2\beta_2\gamma_2$ heterodimer. In addition to MMOH, two other proteins are required for activity in vitro, a 38.5 kDa reductase MMOR, which receives electrons from NADH and then transfers them to MMOH, and a 16 kDa regulatory protein MMOB necessary for efficient catalysis.[7] A range of spectroscopic techniques revealed the existence of intermediates in the reaction of reduced MMOH (H_{red}) with dioxygen in the presence of 2 equiv of MMOB (Scheme 1).[7] The first observable intermediate is H_{peroxo}, which converts rapidly to Q. In the absence of substrates, Q slowly decays to afford oxidized protein (H_{ox}).

Studies of MMOH reactions with substrates other than methane provide valuable information for understanding the hydroxylation mechanism. Reactions employing isotopically labeled substrates allow for the determination of kinetic isotope effects (KIEs), the magnitude of which gives information about the transition state.[8−10] The reactions of Q with CH_4, CH_3CN, and nitromethane exhibit KIEs larger than the theoretical limit for classical mechanisms,[8,9,11] indicating that C−H bond breaking occurs by tunneling at the transition state and is rate-limiting for these reactions. For larger substrates, the KIE approaches 1, and it is postulated that substrate binding or product release becomes rate-limiting.[9−11] Reactions with radical clock substrate probes demonstrate that a discrete radical is not involved in the hydroxylation mechanism.[12] These experimental results, when coupled with recent theoretical studies, have allowed a detailed mechanism to be postulated, based on combined semiclassical molecular dynamics simulations and density functional theoretical calculations, which accounts for many of the observed reactions of MMOH.[12,13] The calculations reveal that Q reacts by two sequential single-electron transfer events.[12,13]

Although the reactivity of Q has been extensively probed, that of H_{peroxo} has not been fully explored. Early indications of multiple oxidizing intermediates in sMMO arose from "peroxide shunt" reactions, in which H_{ox} is activated by hydrogen peroxide in the absence of MMOB.[14] Different product distributions are obtained for these reactions compared to those employing the complete sMMO enzyme system. The greatest difference occurs for reactions with *trans*-2-butene, where the product distribution for the wild-type system revealed 68% alcohol, whereas the peroxide shunt reaction afforded 97% epoxide.[14] This difference could arise from an increase in the activity of the peroxo intermediate compared to that of Q. In addition, sMMO reactions with radical clock substrate probes[15] yield products derived from a cationic intermediate, which were postulated to arise from reaction of a hydroperoxo species with substrate.[12]

The first direct evidence for H_{peroxo} reactivity arose from a stopped-flow optical spectroscopic study carried out in our laboratory, which revealed the decay rate of the peroxo intermediate to increase when exposed to increasing concentrations of propylene.[16] The data covered only a small range of substrate concentration because of the limited solubility of propylene in water, and the differences in the observed rate constants are not large. Using protein isolated from *Mt*, others failed to observe reactions of propylene with H_{peroxo}[17] and suggested that substrate might increase the rate of Q formation. At the low protein and substrate concentrations used in their study, however, the rate constants for reaction with H_{peroxo} would be lower or near the value of peroxo conversion to Q, and consequently, that reaction could not be observed. In addition, they monitored the absorbance change near 420 nm, whereas it is essential to follow reactions of H_{peroxo} at its absorption maximum of 720 nm to avoid interference from Q.

To provide a more definitive assessment of the relative reactivity of the MMOH intermediates with substrates, we have investigated the reactions of ethyl vinyl ether and diethyl ether by single- and double-mixing stopped-flow optical spectroscopy.

(7) Merkx, M.; Kopp, D. A.; Sazinsky, M. H.; Blazyk, J. L.; Müller, J.; Lippard, S. J. *Angew. Chem., Int. Ed.* **2001**, *40*, 2782−2807 and references therein.
(8) Green, J.; Dalton, H. *J. Biol. Chem.* **1989**, *264*, 17698−17703.
(9) Nesheim, J. C.; Lipscomb, J. D. *Biochemistry* **1996**, *35*, 10240−10247.
(10) Brazeau, B. J.; Lipscomb, J. D. *Int. Congr. Ser.* **2002**, *1233*, 229−233.
(11) Ambundo, E. A.; Friesner, R. A.; Lippard, S. J. *J. Am. Chem. Soc.* **2002**, *124*, 8770−8771.
(12) Baik, M.-H.; Newcomb, M.; Friesner, R. A.; Lippard, S. J. *Chem. Rev.* **2003**, *103*, 2385−2419.
(13) (a) Gherman, B. F.; Dunietz, B. D.; Whittington, D. A.; Lippard, S. J.; Friesner, R. A. *J. Am. Chem. Soc.* **2001**, *123*, 3836−3837. (b) Guallar, V.; Gherman, B. F.; Lippard, S. J.; Friesner, R. A. *Curr. Opin. Chem. Biol.* **2002**, *6*, 236−242. (c) Guallar, V.; Gherman, B. F.; Miller, W. H.; Lippard, S. J.; Friesner, R. A. *J. Am. Chem. Soc.* **2002**, *124*, 3377−3384. (d) Baik, M.-H.; Gherman, B. F.; Friesner, R. A.; Lippard, S. J. *J. Am. Chem. Soc.* **2002**, *124*, 14608−14615. (e) Gherman, B. F.; Baik, M.-H.; Lippard, S. J.; Friesner, R. A. *J. Am. Chem. Soc.* **2004**, *126*, 2978−2990. (f) Gherman, B. F.; Lippard, S. J.; Friesner, R. A. *J. Am. Chem. Soc.* **2005**, *127*, 1025−1037.
(14) (a) Andersson, K. K.; Froland, W. A.; Lee, S.-K.; Lipscomb, J. D. *New J. Chem.* **1991**, *15*, 411−415. (b) Jiang, Y.; Wilkins, P. C.; Dalton, H. *Biochim. Biophys. Acta* **1993**, *1163*, 105−112.
(15) Selected references: (a) Dalton, H.; Golding, B. T.; Waters, B. W.; Higgins, R.; Taylor, J. A. *J. Chem. Soc., Chem. Commun.* **1981**, 482−483. (b) Ruzicka, F.; Huang, D.-S.; Donnelly, M. I.; Frey, P. A. *Biochemistry* **1990**, *29*, 1696−1700. (c) Liu, K. E.; Johnson, C. C.; Newcomb, M.; Lippard, S. J. *J. Am. Chem. Soc.* **1993**, *115*, 939−947. (d) Valentine, A. M.; LeTadic-Biadatti, M.-H.; Toy, P. H.; Newcomb, M.; Lippard, S. J. *J. Biol. Chem.* **1999**, *274*, 10771−10776. (e) Choi, S.-Y.; Eaton, P. E.; Kopp, D. A.; Lippard, S. J.; Newcomb, M.; Shen, R. *J. Am. Chem. Soc.* **1999**, *121*, 12198−12199. (f) Jin, Y.; Lipscomb, J. D. *Biochemistry* **1999**, *38*, 6178−6186. (g) Jin, Y.; Lipscomb, J. D. *Biochim. Biophys. Acta* **2000**, *1543*, 47−59. (h) Newcomb, M.; Shen, R.; Lu, Y.; Coon, M. J.; Hollenberg, P. F.; Kopp, D. A.; Lippard, S. J. *J. Am. Chem. Soc.* **2002**, *124*, 6879−6886.
(16) Valentine, A. M.; Stahl, S. S.; Lippard, S. J. *J. Am. Chem. Soc.* **1999**, *121*, 3876−3887.
(17) Brazeau, B. J.; Lipscomb, J. D. *Biochemistry* **2000**, *39*, 13503−13515.

Scheme 2

$$H_{red}{:}2B + O_2 \xrightarrow{k_1} H_{peroxo} \xrightarrow{k_2} Q \xrightarrow{k_3} H_{ox}$$

$$Abs_\lambda(t) = [H_{red}]_0 \left\{ \begin{array}{l} \varepsilon_{H_{ox}} + \left(\left(\varepsilon_{H_{red}} - \varepsilon_{H_{ox}} \right) e^{-k_1' t} \right) + \left(\left(\varepsilon_{H_{peroxo}} - \varepsilon_{H_{ox}} \right) \dfrac{k_1'}{k_2 - k_1'} \left(e^{-k_1' t} - e^{-k_2 t} \right) \right) \\ + \left(\left(\varepsilon_Q - \varepsilon_{H_{ox}} \right) \dfrac{k_2 k_1'}{k_2 - k_1'} \left\{ \dfrac{1}{k_3 - k_1'} \left(e^{-k_1' t} - e^{-k_3 t} \right) - \dfrac{1}{k_3 - k_2} \left(e^{-k_2 t} - e^{-k_3 t} \right) \right\} \right) \end{array} \right\} \quad (1)$$

These molecules have increased solubility and greater nucleophilicity than simple alkanes or alkenes, such as methane and propylene. We derive analytical equations for analyzing the kinetic data obtained from transient kinetic studies of the reactions of H_{peroxo} and Q with these substrates. Activation parameters of the relative rate constants for the two intermediates provide significant insight into the reaction mechanisms, allowing us to conclude unambiguously that H_{peroxo} is reactive, and we propose that it prefers two-electron transfer steps.

Experimental Section

General Considerations. The regulatory (MMOB) and reductase (MMOR) proteins were prepared recombinantly in *Escherichia coli* and purified as described elsewhere.[18] Distilled water was deionized with a Milli-Q filtering system. Diethyl ether was saturated with argon and purified by passing through an activated alumina column under argon. Other reagents were of commercial origin and used as received.

MMOH Purification. Purification of the hydroxylase (MMOH) from native *Methylococcus capsulatus* (Bath) as previously described[19] affords protein that is sometimes contaminated with a small amount of cytochrome that exhibits an absorption band at 410 nm. Protein obtained from this two-step purification procedure typically has a specific activity, as measured for propylene oxidation, in the range of 200−400 mU/mg at 45 °C. Further purification with an Amersham Biosciences MonoQ column allows for separation of MMOH from the cytochrome. Protein eluted from the S-300 size-exclusion column was desalted and concentrated to ca. 150 μM. Between 250 and 350 mg of this concentrated protein was loaded onto a MonoQ column (1 × 8 cm) equilibrated in 25 mM MOPS (pH 7.0) containing 10% glycerol. After the sample was loaded, the column was washed with 10 mL of a 50 mM NaCl solution followed by a linear 200 mL gradient of 0−200 mM NaCl in the same buffer. The hydroxylase eluted from the column at approximately 100 mM NaCl. Hydroxylase-containing fractions were identified by absorbance at 280 nm and SDS−PAGE assays. Pooled fractions were concentrated with an Amicon YM-100 membrane, flash-frozen in liquid nitrogen, and stored at −80 °C. The resulting protein had a specific activity at 45 °C of 400−750 mU/mg, as determined for propylene oxidation.

Stopped-Flow Visible Spectroscopy. Single turnover kinetics experiments were performed on a Hi-Tech Scientific (Salisbury, U.K.) SF-61 DX2 stopped-flow spectrophotometer as described in detail elsewhere.[16] The hydroxylase was reduced with dithionite and methyl viologen in the presence of 2 equiv of MMOB in 25 mM MOPS (pH 7.0) solution, as previously reported.[16] For experiments monitoring reactions of H_{peroxo}, the concentration of H_{red}:2B in the optical cell was 50 μM; otherwise, the concentration was 25 μM. Single-mixing experiments were performed by rapidly mixing the reduced protein solution with a dioxygen-saturated buffered solution. For single-mixing studies in the presence of substrate, the latter was dissolved in the dioxygen-saturated solution. H_{peroxo} and Q are generated by rapidly mixing a fully reduced, anaerobic buffered hydroxylase (H_{red}) solution containing 2 equiv of MMOB with O_2-saturated buffer in the initial push of a double-mixing experiment. After a specified time delay that coincides with maximal concentration of either H_{peroxo} or Q, substrate-containing buffer is introduced in a second push to initiate the reaction.

Scheme 3

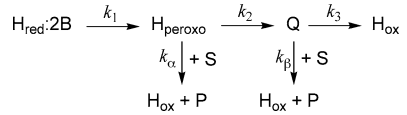

Reactions time courses were monitored at 420 or 720 nm using a photomultiplier detector. Data collection and analysis were performed by using KinetAsyst 3 (Hi-Tech Scientific) and KaleidaGraph v. 3.51 (Synergy Software) software.

Analysis of Stopped-Flow Data. Transient-state kinetic data are typically fit with multiple exponentials and not with analytically derived equations. This procedure yields observed rate constants and amplitudes, each of which is typically assigned to one process. These amplitudes can be complex functions of rate constants, extinction coefficients, and intermediate concentrations. It can be difficult to extract meaningful parameters from them without the use of a full model for the reaction and corresponding mathematical analysis.[20] Therefore, a model based on an A → B → C → D mechanism[21] was modified to account for the ability of B (H_{peroxo}) and C (Q) to react with substrates to give D and products. It is well established that two exponentials differing by a factor of 7 or less cannot be distinguished.[20] Double-mixing experiments were therefore utilized to determine rate constants for the reactions of H_{peroxo} and Q, to obtain initial parameters for use in fitting the single-mixing data for the reactions.

Single-Mixing Experiments. Single-mixing experiments were employed to determine rate constants for the formation and decay of the intermediates and their extinction coefficients. In the absence of substrate, the absorbance versus time ($Abs_\lambda(t)$) curves for reaction of H_{red}:2B with a large excess of O_2 at λ = 420 nm were fit to an A → B → C → D model (Scheme 2) by using eq 1, where $[H_{red}]_0$ is the initial concentration of hydroxylase, ϵ is extinction coefficient for the designated species, and k_1', k_2, and k_3 are rate constants for H_{peroxo} formation, H_{peroxo} conversion to Q, and Q conversion to H_{ox}, respectively. A full derivation of eq 1 is supplied as Supporting Information.

In the presence of substrates that react with H_{peroxo} and Q, $Abs_\lambda(t)$ can be fit to eq 2 based on the model shown in Scheme 3, where $k' = (k_2 + k_\alpha[S])$, the sum of the rate constants for peroxo conversion to Q (k_2) and its reaction with substrate ($k_\alpha[S]$), and $k'' = (k_3 + k_\beta[S])$, the sum of the rate constants for Q conversion to H_{ox} (k_3) and its reaction with substrate ($k_\beta[S]$). A full derivation of eq 2 is given in Supporting Information. It is apparent from eq 2 that determination of the rate constants for the reaction of substrate with H_{peroxo} and Q by single-mixing experiments would be a challenge. However, since the absorption maxima for H_{peroxo} and Q are well separated in energy, and each reaches a maximum concentration at distinct times, it is possible to study the reactions using double-mixing stopped-flow techniques.

(18) (a) Coufal, D. E.; Blazyk, J. L.; Whittington, D. A.; Wu, W. W.; Rosenzweig, A. C.; Lippard, S. J. *Eur. J. Biochem.* **2000**, *267*, 2174−2185. (b) Kopp, D. A.; Gassner, G. T.; Blazyk, J. L.; Lippard, S. J. *Biochemistry* **2001**, *40*, 14932−14941.
(19) Gassner, G. T.; Lippard, S. J. *Biochemistry* **1999**, *38*, 12768−12785.
(20) (a) Pettersson, G. *Acta Chem. Scand. B* **1978**, *32*, 437−446. (b) Fisher, H. F. In *Enzymatic Mechanisms*; Frey, P. A., Northrup, D. B., Eds.; IOS Press: Amsterdam, 1999; pp 264−277.
(21) Szabó, Z. G. In *The Theory of Kinetics*; Bamford, C. H., Tipper, C. F. H., Eds.; Elsevier: New York, 1969; Vol. 2, pp 20−24.

$$Abs_\lambda(t) = [\mathrm{H_{red}}]_0 \left\{ \begin{array}{l} \varepsilon_{\mathrm{H_{ox}}} + \left(\left(\varepsilon_{\mathrm{H_{red}}} - \varepsilon_{\mathrm{H_{ox}}} \right) e^{-k_1' t} \right) + \\ \qquad \left(\left(\varepsilon_{\mathrm{H_{peroxo}}} - \varepsilon_{\mathrm{H_{ox}}} \right) \frac{k_1'}{k' - k_1'} \left(e^{-k_1' t} - e^{-k' t} \right) \right) \\ + \left(\left(\varepsilon_{\mathrm{Q}} - \varepsilon_{\mathrm{H_{ox}}} \right) \frac{k_2 k_1'}{k' - k_1'} \left\{ \frac{1}{k'' - k_1'} \left(e^{-k_1' t} - e^{-k'' t} \right) - \right. \right. \\ \qquad \left. \left. \frac{1}{k'' - k'} \left(e^{-k' t} - e^{-k'' t} \right) \right\} \right) \end{array} \right\} \quad (2)$$

Double-Mixing Experiments. In the absence of substrate, H_{peroxo} decays to Q with rate constant k_2. In the presence of substrate, the data at 720 nm can be fit well with two exponentials, as shown in eq 3, corresponding to the kinetic model of Scheme 4, where A_1 and A_2 are time-independent constants for the corresponding exponentials, $k_{obs1} = k_2 + k_\alpha[S]$ and $k_{obs2} = k_3 + k_\beta[S]$. Reactions of H_{peroxo} with ethyl vinyl ether display a hyperbolic dependence on [S] at low temperature. This behavior may result from a change in protein conformation that precedes substrate oxidation or from the reversible formation of an intermediate:substrate complex. Similar behavior has been observed for the reactions of Q with acetonitrile and nitromethane,[11] and mixed quantum mechanics/molecular mechanics calculations indicate that the behavior is consistent with the formation of a Q:S complex.[13f] Substrate can bind reversibly to H_{peroxo}, forming a complex with the dissociation constant K_d. The complex can react to afford oxidized product with rate constant k_{sat}. At high [S], the peroxo intermediate exists almost entirely as the enzyme−substrate complex. In this limit, k_{obs1} becomes equivalent to k_{sat}. At low [S], the observed rate constant approaches k_2. Simultaneously, H_{peroxo} is converting to Q, which then decays with rate constant k''. Thus, the observed data are fit as a sum of two exponentials, one of which corresponds to the rate constant for Q decay and can be determined in a separate experiment. The other exponential corresponds to H_{peroxo} decay. This explanation is expressed in the model shown in Scheme 5, and the data can be fit to eq 4, where k_{sat} is the rate constant for the reaction of H_{peroxo} with S, and K_d is the dissociation constant for substrate binding to H_{peroxo}. A derivation of eq 4 is given in Supporting Information.

$$\mathrm{Abs}_\lambda(t) = A_1 e^{-k_{obs1} t} + A_2 e^{-k_{obs2} t} + c \quad (3)$$

$$k_{obs1} = k_2 + \frac{k_{sat}[S]}{K_d + [S]} \quad (4)$$

The value of k_β can be determined by double-mixing experiments of Q with substrates at 420 nm. In this case, only a single exponential, which corresponds to k_{obs2} from the 720 nm data, is required to fit the data. After determining the values for the extinction coefficients, k_1', k_2, and k_3, from single-mixing experiments and the values of k_α and k_β from double-mixing experiments, it is possible to fit the data obtained from single-mixing experiments in the presence of substrate.

Determination of Activation Parameters. For a first-order rate constant, the activation parameters for a reaction can be determined by using the Eyring equation (eq 5). The enthalpy of activation ($\Delta H^\ddagger$) for the formation and decay of the intermediates was determined from the slope of a plot of $\ln(k/T)$ versus $1/T$, and the entropy of activation ($\Delta S^\ddagger$) from the slope of a plot of $T\cdot\ln(k/T)$ versus T, where k is k_1', k_2, or k_3. For reactions of the intermediates with substrates, $k_\alpha[S]$ and $k_\beta[S]$ were extracted from the observed rate constants, k_{obs1} and k_{obs2}, by subtracting k_2 and k_3, respectively, and fit to the Eyring equation to obtain $\Delta H^{\ddagger\circ}$ and $\Delta S^\ddagger_{[S]}$, where the entropy of activation is dependent on substrate concentration. To compare activation entropies for second-order reactions, it is necessary to convert the values to the standard entropy of activation ($\Delta S^{\ddagger\circ}$), defined at [S] = 1 M, using eq 6.

Scheme 4

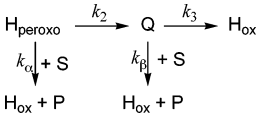

Scheme 5

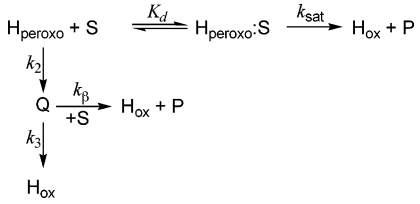

$$k = \frac{k_B T}{h} \exp\left(\frac{-\Delta G^\ddagger}{RT} \right) \quad (5)$$

$$\Delta S^{\ddagger\circ} = \Delta S^\ddagger_{[S]} - R \ln [S] \quad (6)$$

Product Determination. Product formation from steady-state oxidations of diethyl ether and ethyl vinyl ether were monitored by GC and LC−MS, respectively. Solutions of each of the three protein components ([MMOH] = 10 μM; [MMOB] = 20 μM; [MMOR] = 5 μM), NADH, and substrate were prepared in air-saturated 25 mM MOPS (pH 7.0), and the reactions were carried out as described below.

Diethyl Ether. The products of diethyl ether oxidation by sMMO under steady-state conditions using soluble cell extracts were previously determined to be ethanol and acetaldehyde.[22] The use of purified protein components affords the same products, as determined by GC analysis employing a Hewlett-Packard 5890 gas chromatograph. The reactions were carried out in a total volume of 1 mL with 5 mM NADH and 5 mM diethyl ether at 45 °C. After 0 and 15 min, aliquots of the reaction solution (5 μL) were injected onto an Alltech Porapak Q column (6' × $^1/_8$") equilibrated at 60 °C. After 10 min, the temperature was ramped at 10 °C/min to 160 °C. Under these conditions, authentic samples of acetaldehyde, ethanol, and diethyl ether exhibited retention times of 15.9, 19.6, and 21.4 min, respectively. Under the same conditions, in the absence of NADH, no ethanol or acetaldehyde was detected. Representative GC traces are shown in Figure S1 (Supporting Information).

Ethyl Vinyl Ether. GC analysis of ethyl vinyl ether reactions is complicated because the substrate decomposes on the column. Therefore, analysis of the reaction was carried out in a manner similar to that used for the reaction of *p*-nitrophenyl vinyl ether with microsomal P450.[23] The steady-state reaction was carried out in 0.5 mL containing 2 mM NADH and 2 mM ethyl vinyl ether at 20 °C. After 20 min, the reaction was terminated by addition of 100 μL of 6 mM 2,4-dinitrophenylhydrazine (2,4-DNPH) dissolved in 6 M HCl. The solution was heated at 100 °C for 30 min to ensure conversion of the aldehyde products to their corresponding hydrazones, which were extracted into benzene (200 μL). Aliquots (100 μL) of the benzene solution were dried, and the solid residue was dissolved in 100 μL of methanol and analyzed by HPLC. The analysis was performed using an Agilent 1100 series LC/MSD trap equipped with a VYDAC C-18 reverse-phase column with methanol:water (3:2) as the mobile phase. Under these conditions, 2,4-DNPH, glycolaldehyde-2,4-dinitrophenylhydrazone, and acetaldehyde-2,4-dinitrophenylhydrazone eluted at 7.1, 10.0, and 13.3 min, respectively. The identity of each substance was determined by

(22) Colby, J.; Stirling, D. I.; Dalton, H. *Biochem. J.* **1977**, *165*, 395−402.
(23) Isobe, M.; Sone, T.; Takabatake, E. *J. Phamacobio-Dyn.* **1985**, *8*, 614−622.

Table 1. Extinction Coefficients for Intermediates Observed in the Reaction of H_{red}:2B with Dioxygen

species	ϵ_{420} (M^{-1} cm^{-1})
H_{red}:2B	3200
H_{peroxo}	4600
Q	9850
H_{ox}	3400 ± 200

comparison to hydrazones prepared from authentic glycolaldehyde dimer and acetaldehyde.

Results

Analysis of the products from the steady-state reaction of ethyl vinyl ether reveals ethanol, glycolaldehyde, and acetaldehyde. The acetaldehyde is formed by acid-catalyzed decomposition of ethyl vinyl ether, which also produces ethanol. The epoxidation product is unstable, and its decomposition yields ethanol and glycolaldehyde; thus, both intermediates epoxidize the double bond. The instability of epoxides of alkyl vinyl ethers in water and their decomposition to glycolaldehyde and the corresponding alcohol have been previously reported.[24] The other possible products are ethylene glycol vinyl ether, which was not observed by GC analysis, and the hemiacetal resulting from hydroxylation at the α-carbon atom of the ethyl group, which would rapidly decompose to afford 2 equiv of acetaldehyde.

The products of the steady-state oxidation of diethyl ether were previously determined by whole cell assays to be ethanol and acetaldehyde, produced by decomposition of the hemiacetal formed upon hydroxylation at the α-carbon of diethyl ether. Analysis of the products from steady-state reactions employing purified enzyme components reveals ethanol and acetaldehyde, as previously reported.[22] The other possible product, ethylene glycol ethyl ether, was not observed by GC analysis.

Intermediate Formation and Decay in the Absence of Substrates. The optical spectra of the intermediates observed upon reaction of H_{red}:2B with dioxygen have been reported previously.[16] The peroxo intermediate exhibits broad absorption bands centered at 420 nm ($\epsilon = 4600$ M^{-1} cm^{-1}) and 720 nm ($\epsilon \approx 2000$ M^{-1} cm^{-1}), and intermediate Q displays a broad absorption centered at 420 nm ($\epsilon = 9850$ M^{-1} cm^{-1}) that tails into the NIR with an extinction coefficient of $\epsilon \approx 1000$ M^{-1} cm^{-1} at 720 nm. The extinction coefficient for H_{ox}:2B was determined by using a known concentration of protein, and the values for H_{red}, H_{peroxo}, and Q were determined by fitting to eq 1 (Table 1). The activation parameters for the formation of H_{peroxo}, conversion of H_{peroxo} to Q, and conversion of Q to H_{ox} were determined from fitting the reaction time courses obtained at 420 and 720 nm to an A → B → C model (Table 2); the results agree well with published values.[16] In the absence of substrate, formation and decay of the peroxo intermediate were determined to be 9.8 and 10 s^{-1} at 20 °C and 1.6 and 0.40 s^{-1} at 4 °C, respectively. The formation of Q, monitored at 420 nm, is equal to the rate of peroxo decay, and the rate constant for Q decay is 0.12 and 0.05 s^{-1} at 20 and 4 °C, respectively. Correspondingly, the concentration of H_{peroxo} maximizes at ca. 40 ms and 1 s at 20 and 4 °C, respectively, and the concentration of Q at ca. 500 ms and 8 s at 20 and 4 °C, respectively. Thus, we monitored the reactions of substrates at 4 °C because the smaller rate constants allowed for the collection of more data points and reduced noise in double-mixing stopped-flow visible spectroscopic experiments.

Table 2. Activation Parameters for Formation and Decay of Intermediates Observed in the Reaction of H_{red}:2B with Dioxygen in 25 mM MOPS (pH 7)

rate constant[a]	$\Delta H^{\ddagger}$ (kcal/mol)	$\Delta H^{\ddagger}$ [b] (kcal/mol)	$\Delta S^{\ddagger}$ (cal/mol·K)	$\Delta S^{\ddagger}$ [b] (cal/mol·K)
k_1'	27.9 ± 0.1	22 ± 4	43 ± 2	21 ± 10
k_2	28.7 ± 0.3	29 ± 1	43.9 ± 0.5	45 ± 3
k_3	13.7 ± 0.7	14 ± 1	−18 ± 2	−15 ± 3

[a] Values of k_1', k_2, and k_3 refer to H_{peroxo} formation, H_{peroxo} conversion to Q, and Q conversion to H_{ox}, respectively. [b] Values from ref 16.

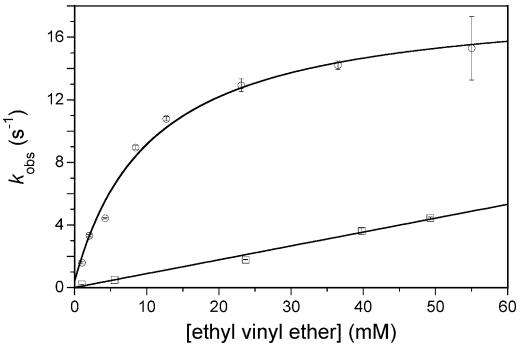

Figure 1. Plot of k_{obs} versus ethyl vinyl ether concentration for the decay of H_{peroxo} (circles) and Q (squares) obtained from double-mixing experiments at 4 °C and pH 7. A linear fit to the data for reaction with Q reveals a second-order rate constant of 88.6 ± 0.3 M^{-1} s^{-1}, and a fit of the data for the reaction with H_{peroxo} to eq 4 reveals $k_{sat} = 18.1 \pm 0.8$ s^{-1} and $K_d = 11 \pm 1$ mM.

Reactions with Ethyl Vinyl Ether. Previous work revealed that the decay rate of Q is accelerated in the presence of substrates,[16,25] and that the rate constant for this process is equal to that for substrate loss,[26] but only one such example has been provided for H_{peroxo}, its reaction with propylene.[16] In this double-mixing experiment, the decay rate of H_{peroxo} increased with increasing concentrations of propylene; however, the change in peroxo decay rates was small because of the limited solubility of propylene. Thus, we decided to explore reactions with the more soluble, electron-rich olefin ethyl vinyl ether. The second-order rate constant at 4 °C obtained for reaction of ethyl vinyl ether with Q is 88.6 ± 0.3 M^{-1} s^{-1} (Figure 1). The plot of k_{obs1} versus [S] for reaction with H_{peroxo} at 4 °C exhibits a hyperbolic dependence on [S], and for all substrate concentrations, the observed rate constant for reaction with H_{peroxo} is greater than that for Q, providing convincing evidence that H_{peroxo} does react with olefins. The data were fit to eq 4 using the model shown in Scheme 5, with k_2 set at 0.4 s^{-1} to give a rate constant k_{sat} of 18.1 ± 0.8 s^{-1} and dissociation constant K_d of 11 ± 1 mM. At 20 °C, reactions with both intermediates display linear dependencies on [S], yielding second-order rate constants of 1500 ± 100 M^{-1} s^{-1} for H_{peroxo} and 223 ± 10 M^{-1} s^{-1} for intermediate Q. These rate constants and those for the reaction of other substrates with both intermediates are reported in Table 3. The time traces for the reactions at 20 °C are presented in Figures S2 and S3 (Supporting Information).

(24) Sone, T.; Isobe, M.; Takabatake, E. *Chem. Pharm. Bull.* **1989**, *37*, 1922−1924.
(25) Liu, Y.; Nesheim, J. C.; Lee, S.-K.; Lipscomb, J. D. *J. Biol. Chem.* **1995**, *270*, 24662−24665.
(26) Muthusamy, M.; Ambundo, E. A.; George, S. J.; Lippard, S. J.; Thorneley, R. N. F. *J. Am. Chem. Soc.* **2003**, *125*, 11150−11151.

Table 3. Rate Constants for the Reactions of Ethers and Propylene with H_{peroxo} and Q Obtained from Double-Mixing Experiments

substrate	species	T (°C)	k ($M^{-1}s^{-1}$)	k_{sat} (s^{-1})	K_d (mM)
propylene[a]	H_{peroxo}	20.0	3400 ± 200		
	Q	20.0	12000		
ethyl vinyl ether	H_{peroxo}	4.0		18.1 ± 0.8	11 ± 1
	Q	4.0	88.6 ± 0.3		
	H_{peroxo}	20.0	1,500 ± 200		
	Q	20.0	223 ± 10		
diethyl ether	H_{peroxo}	4.0	17 ± 1		
	Q	4.0	2.2 ± 0.1		
diethyl ether-d_{10}	H_{peroxo}	4.0	8.7 ± 0.1		
	Q	4.0	1.59 ± 0.5		

[a] Data taken from ref 16.

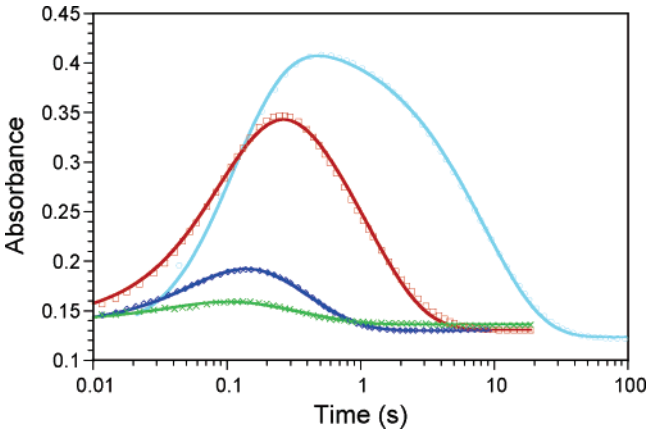

Figure 2. Plot of the evolution in absorbance at 420 nm after mixing H_{red}:2B with buffer containing dioxygen and ethyl vinyl ether at 20 °C and pH 7. The concentration of ethyl vinyl ether was 0 (cyan), 1.14 (red), 5.7 (blue), and 13.2 (green) mM. For [S] = 0, the data were fit to eq 1 using the extinction coefficients listed in Table 1 to afford k_1' of 40, k_2 of 9.8, and k_3 of 0.12 s^{-1}. These rate constants were then used to fit the data obtained in the presence of substrate to eq 2. This procedure yielded values of k_α[S] = 10.37 ± 0.01, 15.8 ± 0.1, and 26.3 ± 0.6 s^{-1} and the values of k_β[S] = 0.906 ± 0.006, 2.81 ± 0.02, and 2.81 ± 0.6 s^{-1} for [S] = 1.14, 5.7, and 13.2 mM, respectively.

Single-mixing experiments in the presence of substrate were carried out to verify that the dependence of k_{obs1} on [S] was not due solely to an increased value for k_2. Fits of the evolution of the absorbance at 420 nm after mixing H_{red}:2B with dioxygen and increasing concentrations of substrate fit to the model shown in Scheme 3 using eq 2 reveal that H_{peroxo} is reacting with substrate and converting directly to H_{ox} instead of Q. This behavior results in the maximum value of the absorbance decreasing, and the maximum occurring at an earlier time, with increasing substrate concentration (Figure 2). If the dependence of k_{obs1} on [S] were due solely to an increased value for k_2, a similar shift would be observed and the single-mixing data could be fit to eq 1. However, the results from such a fit require a value of k_2 twice that observed in double-mixing experiments (Figure 3). In addition, the fit using eq 1 affords larger residuals compared to the fit using eq 2. If the value of k_2 was set to the value of k_α[S] determined from double-mixing experiments, the fit was even less satisfying. A dramatic decrease in the extinction coefficient for Q is required because eq 1 does not account for the conversion of H_{peroxo} directly to H_{ox}, which reduces the absorption maximum at 420 nm due to the lower extinction coefficients for these species compared to that for Q. The percentage of H_{peroxo} converting to Q is equal to (k_2/k_{obs1}) such that, at high values of [S], very little Q is formed. Thus, the

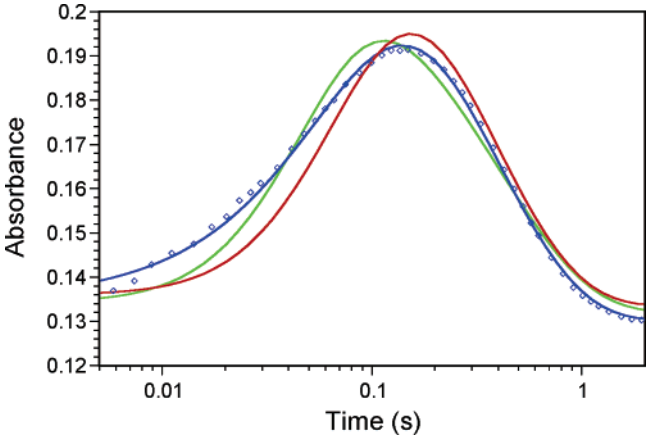

Figure 3. Plot of the evolution in absorbance at 420 nm after mixing H_{red}:2B with buffer containing dioxygen and 5.7 mM ethyl vinyl ether at 20 °C and pH 7. The blue line is a fit to eq 2 using the parameters given in Figure 2. The green line is a fit to the data using eq 1, where k_2 is allowed to vary. The value of 39 s^{-1} is nearly twice that observed in double-mixing experiments. The red line is generated by fitting the data to eq 1 with k_2 set at 18 s^{-1}.

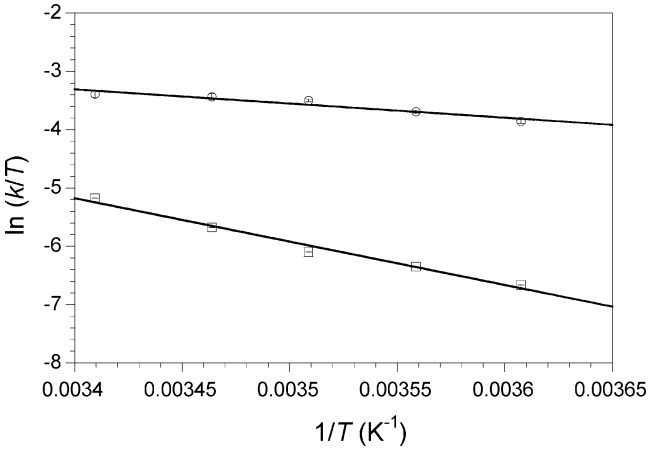

Figure 4. Eyring plots for reaction of H_{peroxo} (circles) and Q (squares) with 4.16 mM ethyl vinyl ether obtained from double-mixing experiments at pH 7.

Table 4. Activation Parameters for the Reactions of H_{peroxo} and Q with Ethers

substrate	[S] (mM)	intermediate	$\Delta H^\ddagger$ (kcal/mol)	$\Delta S^\ddagger$ (cal/mol·K)	$\Delta S^{\ddagger o}$ [a] (cal/mol·K)
ethyl vinyl ether	4.16	H_{peroxo}	4.8 ± 0.8	−40 ± 10	−30 ± 7
	4.16	Q	15 ± 1	−6.5 ± 0.7	3.9 ± 0.4
diethyl ether	75.0	H_{peroxo}	12.6 ± 0.9	−12 ± 1	−7.1 ± 0.6
	75.0	Q	19.5 ± 0.4	8.7 ± 0.2	13.6 ± 0.3
diethyl ether-d_{10}	75.0	H_{peroxo}	14 ± 3	−8 ± 2	−3.1 ± 0.8
	75.0	Q	21.0 ± 0.3	13.8 ± 0.2	18.7 ± 0.3

[a] Calculated using eq 6.

increased rate constant for H_{peroxo} decay cannot be ascribed to a larger value of k_2 alone. The temperature dependence of H_{peroxo} and Q decay in the presence of substrate was monitored at 720 and 420 nm, respectively. Linear Eyring plots (Figure 4) were obtained for both intermediates, and the extracted activation parameters are given in Table 4.

Reactions with Diethyl Ether. For the reaction with diethyl ether, both intermediates exhibit linear dependencies on [S] (Figure 5), and the second-order rate constants are 17 ± 1 and 2.2 ± 0.1 M^{-1} s^{-1} for H_{peroxo} and Q (Table 3), respectively. For reactions with perdeuterated diethyl ether, the second-order

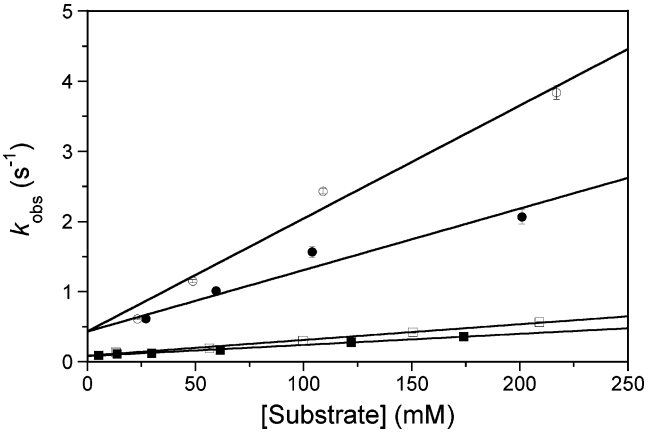

Figure 5. Substrate concentration dependence of the kinetics of the optical decay for H_{peroxo} at 720 nm (circles) and for Q at 420 nm (squares) obtained from double-mixing experiments with diethyl ether (open) and perdeuterated diethyl ether (filled) at pH 7 and 4 °C.

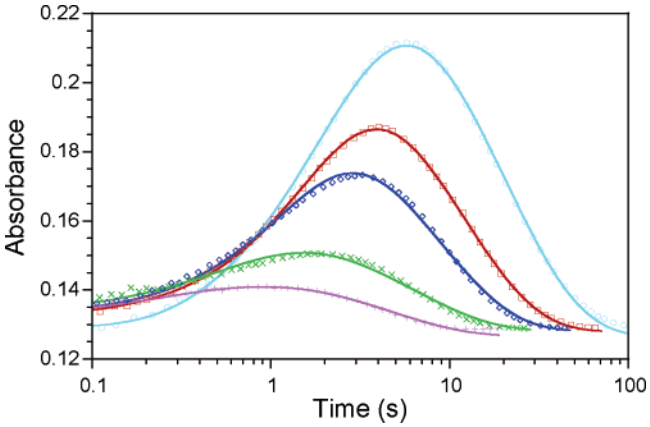

Figure 6. Plot of the evolution in absorbance at 420 nm after mixing H_{red}:2B with buffer containing dioxygen and diethyl ether at 4 °C and pH 7. The concentration of diethyl ether was 0 (cyan), 23 (red), 51 (blue), 107 (green), and 196 (purple) mM. In the absence of diethyl ether, the data were fit to eq 1 using the extinction coefficients listed in Table 1 to afford k_1' of 1.6, k_2 of 0.46, and k_3 of 0.05 s^{-1}. These rate constants were then used to fit the data obtained in the presence of substrate to eq 2. This procedure yielded values of $k_\alpha[S] = 0.192$, 0.5, 2.12, and 4.04 s^{-1} and the values of $k_\beta[S] = 0.0384$, 0.069, 0.107, and 0.17 s^{-1} for [S] = 23, 51, 107, and 196 mM, respectively.

rate constants are 8.7 ± 0.1 and 1.59 ± 0.05 s^{-1} for H_{peroxo} and Q, respectively. The values for the KIE, k_H/k_D, are 2.0 ± 0.2 and 1.4 ± 0.3 for H_{peroxo} and Q, respectively. The time traces for the reaction of H_{peroxo} with diethyl ether are presented in Figure S4 (Supporting Information).

Single-mixing experiments in the presence of substrate were performed in a manner similar to that for ethyl vinyl ether, and the same general features were observed (Figure 6). A fit of the evolution of the absorbance at 420 nm to eq 2 supports the proposed reaction scheme (Scheme 3). Again, eq 1 does not adequately fit the data (Figure 7). The temperature dependence of H_{peroxo} and Q decay in the presence of substrate was monitored at 720 and 420 nm, respectively. Linear Eyring plots (Figure 8) were obtained for both intermediates, and the extracted activation parameters are given in Table 4.

Discussion

Intermediates in the MMOH Catalytic Cycle. The activation parameters obtained for formation and decay of the

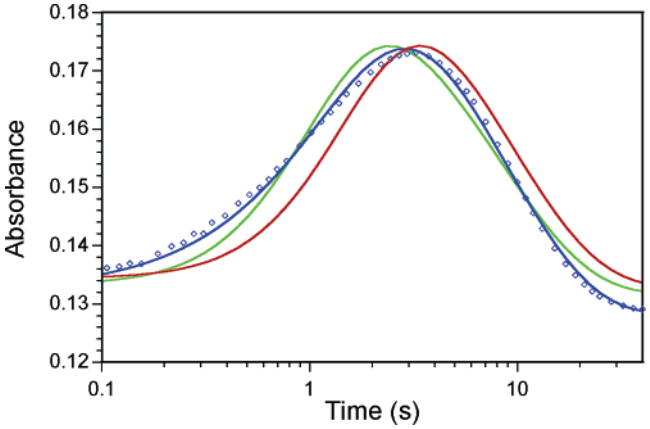

Figure 7. Plot of the evolution in absorbance at 420 nm after mixing H_{red}:2B with buffer containing dioxygen and 51 mM diethyl ether at 4 °C and pH 7. The blue line is a fit to eq 2 using the parameters given in Figure 6. The green line is a fit to the data using eq 1, where k_2 is allowed to vary. The value of 2.12 s^{-1} is nearly twice that observed in double-mixing experiments. The red line is generated by fitting the data to eq 1 with k_2 set at 1 s^{-1}.

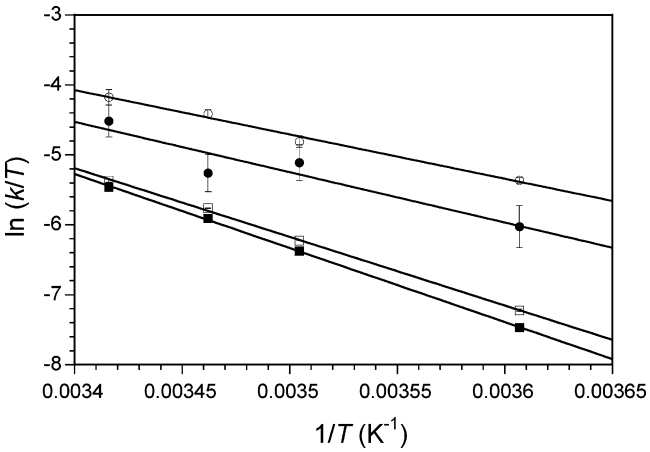

Figure 8. Eyring plots for reaction of H_{peroxo} (circles) and Q (squares) with 75 mM diethyl ether (open symbols) and diethyl ether-d_{10} (filled symbols) obtained from double-mixing experiments at pH 7.

oxygenated intermediates in MMOH agree well with those found in earlier work.[16,27] The large entropy of activation for conversion of peroxo to Q means that the activation free energy is highly temperature-dependent and highlights the importance of studying reactions of H_{peroxo} at 4 °C.

The structure of H_{peroxo} is not established because it has not been possible to obtain its resonance Raman spectrum. Recent calculations from our group and others indicate an η^2:η^2 butterfly structure to be energetically most favorable,[12,13,28] although others prefer a μ-1,2 structure based on theoretical studies and comparison with other diiron proteins.[29] For example, the resonance Raman spectroscopy reveals that the peroxo intermediates observed for stearoyl−acyl carrier protein Δ^9-desaturase,[30] ferritin,[31] and mutants of ribonucleotide reductase R2[29,32] have μ-1,2 bridging peroxo ligands. However, it is not

(27) Recent work in our lab indicates that MOPS is a substrate for MMO and that the reported activation parameters may be those for reaction of the intermediates with MOPS. Further studies are underway to determine the role of buffer in transient studies of MMOH. Beauvais, L. G.; Lippard, S. J., unpublished work.
(28) (a) Siegbahn, P. E. M. *J. Biol. Inorg. Chem.* **2001**, *6*, 27−45. (b) Siegbahn, P. E. M. *Chem. Phys. Lett.* **2002**, *351*, 311−318.
(29) Skulan, A. J.; Brunold, T. C.; Baldwin, J.; Saleh, L.; Bollinger, J. M., Jr.; Solomon, E. I. *J. Am. Chem. Soc.* **2004**, *126*, 8842−8855.

surprising that the structure of the peroxo intermediate would be different for MMOH compared to these other diiron proteins because MMOH is the only system in which a diiron(IV) intermediate has been observed. Thus, the side-on bridging butterfly structure may be necessary for homolytic O−O bond cleavage to afford Q, whereas the μ_1,μ_2 end-on bridged structure might lead to heterolytic O−O bond cleavage. In fact, recent work on diiron model complexes that form (μ-1,2-peroxo)-diiron(III) intermediates suggests that these species are not very reactive and may not be involved in the dioxygen activation pathway of MMOH.[33] Moreover, butterfly peroxo structures are common for dicopper enzymes and react in an electrophilic manner, whereas di(μ-oxo)dicopper(III) species prefer one-electron transfer mechanisms.[34] These studies revealed that the (μ-η^2:η^2-peroxo)dicopper(II) complexes are much more electrophilic than the oxo species. The barrier to conversion between these two intermediates can be very small, such that they are in equilibrium in solution.[34,35] In contrast, the free energy of H_{peroxo} in MMOH is calculated to be 9.8 kcal/mol higher than that of Q and 54.5 kcal/mol higher than that of H_{ox};[12,13d,e] thus, there is a large driving force for H_{peroxo} both to react with substrates and to convert to Q.

Epoxidation of Ethyl Vinyl Ether. It was previously determined that the second-order rate constant for reaction of H_{peroxo} with propylene to form exclusively propylene oxide was ca. 5 times less than that with Q.[16] Upon switching to the more electron-rich olefin ethyl vinyl ether investigated here, the reaction is even faster with H_{peroxo} than with Q. By what mechanism can these results be rationalized? Mayr and co-workers determined a scale of nucleophilicity (*N*) for a wide range of compounds according to their reactions with various electrophiles, where a larger value of *N* indicates greater nucleophilicity. On this scale, the *N* values are −2.41 and 3.92 for propylene and diethyl ether, respectively.[36] H_{peroxo} thus appears to be a more electrophilic oxidant because it reacts with a rate constant significantly larger than that of Q with the more nucleophilic substrate.

Proposed mechanisms for olefin epoxidation are depicted in Figure 9. Intermediate Q is expected to react by two single-electron transfer steps, according to our previous analysis, to afford a bound radical intermediate.[12,13e,f] H_{peroxo} could react by a concerted mechanism or by two-electron transfer to afford a cationic intermediate, which would be stabilized for ethyl vinyl ether by the oxonium resonance structure (Figure 9). Such stabilization would not be available for propylene, and thus its reactions would have a higher energy barrier. The stabilization of an oxonium transition state would be consistent with the lower activation enthalpy observed for H_{peroxo} versus Q, and the more ordered transition state would explain the large negative entropy of activation.

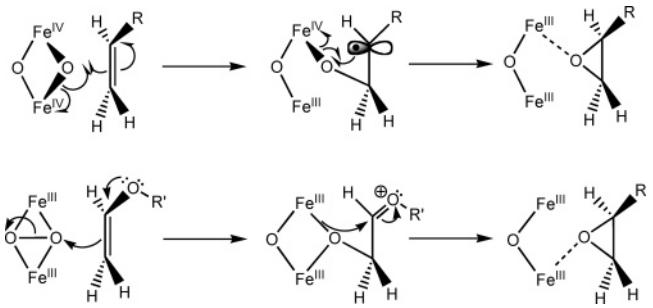

Figure 9. Proposed mechanism for the reactions of Q (top) and H_{peroxo} (bottom) with olefins. Note that the reaction with Q proceeds via two single-electron transfer steps, and the reaction with H_{peroxo} occurs via two-electron transfer steps to afford a cationic intermediate. The oxonium intermediate stabilizes the transition state for the reaction with H_{peroxo} and leads to a much lower activation energy compared to that for Q.

Hydroxylation of Diethyl Ether. The second-order rate constant for reaction of diethyl ether with H_{peroxo} is larger than that observed for Q. The homolytic C−H bond dissociation energies for the methylene and methyl C−H bonds of diethyl ether are 89 and 112 kcal/mol, respectively, as determined from the C−H stretching overtone spectra. Given these values, it is not surprising that sMMO reacts only at the α-C−H bond.[37] Additionally, the gas-phase heterolytic bond dissociation energy $D(R^+H^-)$ of diethyl ether has been calculated to be 214 kcal/mol,[38] indicating that abstraction of hydride ions from this substrate is facile. A more useful parameter for solution phase experiments is the solution hydride affinity $\Delta G_{hydride}(R^+)_s$, which can be estimated as 95 kcal/mol using eq 7.[39] Thus, $H^\bullet$ and H^- abstractions from diethyl ether have comparable energetic barriers. Indeed, gas-phase reactions of diethyl ether with FeH^+ occur via hydride abstraction,[38] and the mechanism for the oxidation of ethers with bromide, permanganate, and Hg(II) has been assigned to a hydride transfer mechanism.[40] More importantly, reactions of aqueous Fe(IV) species with ethers are believed to proceed by both hydrogen atom and hydride abstraction.[41]

$$\Delta G_{hydride}(R^+)_s = 0.904D(R^+H^-) - 98.7 \qquad (7)$$

The proposed mechanism is shown in Figure 10. Intermediate Q reacts by two single-electron transfers, which gives a bound radical intermediate as for methane.[12,13e,f] Comparing the activation parameters for diethyl ether with those for these other substrates, and their solution phase ionization potentials, reveals Et_2O to have a much higher enthalpy of activation (Table 5). Given the low calculated solution phase ionization potentials, it may first transfer an electron and then a proton, in contrast

(30) (a) Broadwater, J. A.; Ai, J.; Loehr, T. M.; Sanders-Loehr, J.; Fox, B. G. *Biochemistry* **1998**, *37*, 14664−14671. (b) Broadwater, J. A.; Achim, C.; Münck, E.; Fox, B. G. *Biochemistry* **1999**, *38*, 12197−12204. (c) Lyle, K. S.; Moënne-Loccoz, P.; Ai, J.; Sanders-Loehr, J.; Loehr, T. M.; Fox, B. G. *Biochemistry* **2000**, *39*, 10507−10513.
(31) Moënne-Loccoz, P.; Krebs, C.; Herlihy, K.; Edmondson, D. E.; Theil, E. C.; Huynh, B. H.; Loehr, T. M. *Biochemistry* **1999**, *38*, 5290−5295.
(32) (a) Moënne-Loccoz, P.; Baldwin, J.; Ley, B. A.; Loehr, T. M.; Bollinger, J. M., Jr. *Biochemistry* **1998**, *37*, 14659−14663. (b) Baldwin, J.; Voegtli, W. C.; Khidekel, N.; Moënne-Loccoz, P.; Krebs, C.; Pereira, A. S.; Ley, B. A.; Huynh, B. H.; Loehr, T. M.; Riggs-Gelasco, P. J.; Rosenzweig, A. C.; Bollinger, J. M., Jr. *J. Am. Chem. Soc.* **2001**, *123*, 7017−7030.
(33) Kryatov, S. V.; Taktak, S.; Korendovych, I. V.; Rybak-Akimova, E. V.; Kaizer, J.; Torelli, S.; Shan, X.; Mandal, S.; MacMurdo, V. L.; Mairata i Payeras, A.; Que, L., Jr. *Inorg. Chem.* **2005**, *44*, 85−99.
(34) (a) Pidcock, E.; Obias, H. V.; Zhang, C. X.; Karlin, K. D.; Solomon, E. I. *J. Am. Chem. Soc.* **1998**, *120*, 7841−7847. (b) Henson, M. J.; Mukherjee, P.; Root, D. E.; Stack, T. D. P.; Solomon, E. I. *J. Am. Chem. Soc.* **1999**, *121*, 10332−10345. (c) Shearer, J.; Zhang, C. X.; Hatcher, L. Q.; Karlin, K. D. *J. Am. Chem. Soc.* **2003**, *125*, 12670−12671.
(35) Cramer, C. J.; Smith, B. A.; Tolman, W. B. *J. Am. Chem. Soc.* **1996**, *118*, 11283−11287.
(36) Mayr, H.; Kempf, B.; Ofial, A. R. *Acc. Chem. Res.* **2003**, *36*, 66−77.
(37) Fang, H. L.; Meister, D. M.; Swofford, R. L. *J. Phys. Chem.* **1984**, *88*, 410−416.
(38) Halle, L. F.; Klein, F. S.; Beauchamp, J. L. *J. Am. Chem. Soc.* **1984**, *106*, 2543−2549.
(39) This relationship was originally determined for aromatic species but should yield a decent approximation for nonaromatic systems. Cheng, J.-P.; Handoo, K. L.; Parker, V. D. *J. Am. Chem. Soc.* **1993**, *115*, 2655−2660.
(40) Barter, R. M.; Littler, J. S. *J. Chem. Soc. B* **1967**, 205−210.
(41) Pestovsky, O.; Bakac, A. *J. Am. Chem. Soc.* **2004**, *126*, 13757−13764.

Table 5. Comparison of Activation Parameters for Reactions of Q with Various Substrates and Their Calculated Solution Phase Ionization Potential (I')

substrate	$\Delta H^{\ddagger}$ (kcal/mol)	$\Delta S^{\ddagger}$[b] (cal/mol·K)	I'[c] (eV)
methane[a]	8.5 ± 0.3	−9.6 ± 0.4	
ethane[a]	15.1 ± 0.2	12 ± 0.7	
ethane-d_6[a]	13.3 ± 0.1	6.5 ± 0.4	
MeCN[a]	11.7 ± 0.1	−6.2 ± 0.2	9.35
MeCN-d_3[a]	11.1 ± 0.2	−13.5 ± 0.4	
$MeNO_2$[a]	11.2 ± 0.1	−10.7 ± 0.3	8.64
$MeNO_2$-d_3[a]	14.3 ± 0.2	−4.4 ± 0.3	
CH_3OH[a]	14.3 ± 0.2	3.5 ± 0.4	7.25
CD_3OD[a]	14.1 ± 0.2	2.7 ± 0.3	
Et_2O	19.5 ± 0.4	13.6 ± 0.3	6.79
Et_2O-d_{10}	21.0 ± 0.3	18.7 ± 0.3	

[a] Data from ref 11. [b] Calculated using eq 6. [c] Values from ref 42.

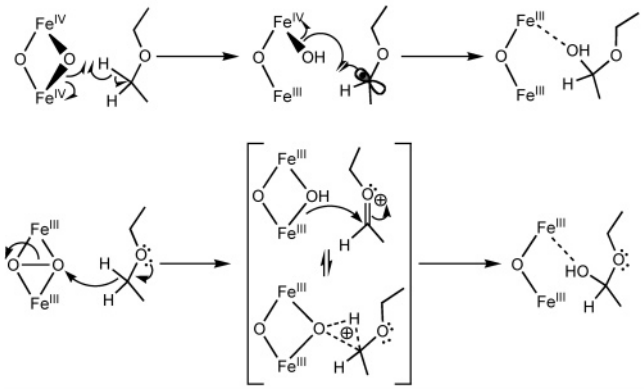

Figure 10. Proposed mechanism for the hydroxylation of diethyl ether by Q (top) and H_{peroxo} (bottom). Note that the intermediate for the reaction with H_{peroxo} has two resonance forms, a 3c−2e$^-$ species and an oxonium species.

to substrates having higher ionization potentials.[42] This mechanism would explain the low value of the KIE because electron transfer would be the rate-limiting step. Alternatively, the true KIE would be obscured if substrate binding were rate-limiting.

The peroxo intermediate could react by two-electron transfer to afford either a cationic or a 3c−2e$^-$ intermediate, which would be stabilized for diethyl ether due to the oxonium resonance structure (Figure 10). Low values of KIE for hydride transfer reactions are not uncommon, and they typically arise from the geometry of the transition state.[43] Thus, the value of 2.0 does not preclude hydride transfer as the rate-limiting step. For example, hydride abstraction from benzyl alcohols by methyltrioxorhenium has a KIE of 3.2.[44] In addition, a hydride abstraction mechanism would explain the presence of products arising from cationic intermediates found for the steady-state reaction of radical clock substrate probes with sMMO.[12,13]

Conclusions and Predictions

Stopped-flow experiments have provided insight into the reactivity of H_{peroxo} and Q with olefins and diethyl ether. The data indicate that the peroxo intermediate of sMMO is more electrophilic than Q and suggest that H_{peroxo} reacts by a two-electron transfer mechanism. The greater reactivity of the peroxo intermediate is consistent with its higher calculated free energy. Density functional theoretical work indicates a (μ-η^2:η^2-peroxo)-diiron(III) structure to be the preferable geometry for H_{peroxo}, and the related species is also highly electrophilic for related dicopper(II) systems. The greater charge of a diiron(III) compared to that of a dicopper(II) center may further activate H_{peroxo}, increasing its electrophilicity. In addition, the oxo-bridged dimetallic intermediates in sMMO and dicopper models prefer one-electron transfer steps.

The present work suggests that H_{peroxo} should react with alcohols and aldehydes, which have low heterolytic bond dissociation energies. Further work with reporter substrates capable of differentiating between one- and two-electron reactions, such as norcarane, cyclobutanol, and methylcyclopropane, is required to test this hypothesis. Moreover, we propose that the electrophilicity of H_{peroxo} can be further revealed by examination of additional olefins of varying nucleophilicity.[36] Finally, this study demonstrates that the reactions of multiple intermediates in an enzyme system can be deconvoluted using stopped-flow optical spectroscopy, and extensions to other bacterial multicomponent monooxygenases would be of interest for systems in which the intermediates can be accessed.

Acknowledgment. This work was supported by NIH Grant GM32134. L.G.B. is a Postdoctoral Trainee under NCI Cancer Training Grant CA09112. We thank J. Bautista for experimental assistance, and Prof. J. P. Sadighi, Prof. R. A. Friesner, Mr. L. J. Murray, and Dr. D. Rinaldo for helpful discussions.

Supporting Information Available: Derivations of eqs 1, 2, and 4, and Figures S1−S4 as described in the text (PDF). This material is available free of charge via the Internet at http://pubs.acs.org.

JA050865I

(42) Pearson, R. G. *J. Am. Chem. Soc.* **1986**, *108*, 6109−6114.
(43) (a) Kwart, H. *Acc. Chem. Res.* **1982**, *15*, 401−408. (b) McLennan, D. J.; Gill, P. M. W. *J. Am. Chem. Soc.* **1985**, *107*, 2971−2972.
(44) Zauche, T. H.; Espenson, J. H. *Inorg. Chem.* **1998**, *37*, 6827−6831.